European Journal of Medicinal Chemistry 119 (2016) 83–95

Contents lists available at ScienceDirect

European Journal of Medicinal Chemistry

journal homepage: http://www.elsevier.com/locate/ejmech

Research paper

Design, synthesis and biological evaluation of novel HSP70 inhibitors: N, N′-disubstituted thiourea derivatives

Yan-qun Zeng [a, b], Rui-yuan Cao [a, **], Jian-ling Yang [a], Xing-zhou Li [a], Song Li [a], Wu Zhong [a, *]

[a] Laboratory of Computer-Aided Drug Design and Discovery, Beijing Institute of Pharmacology and Toxicology, 27 Taiping Rd., Beijing 100850, China
[b] Shenyang Pharmaceutical University, Shenyang, Liaoning, 110016, China

ARTICLE INFO

Article history:
Received 16 October 2014
Received in revised form
14 April 2016
Accepted 15 April 2016
Available online 20 April 2016

Keywords:
Anti-cancer
HSP70 inhibitors
SPR
Synergism
Combinatorial drug therapy

ABSTRACT

As novel heat shock protein 70 (HSP70) inhibitors, N, N′-disubstituted thiourea derivatives were designed and synthesized based on the X-ray structure of the ATPase domain (nucleotide binding domain, NBD). An ATPase activity inhibition assay revealed that these compounds effectively inhibited HSP70 ATPase activity. The results revealed that the compounds 370/371/374/379/380//392/394/397/404/405 and 407 can inhibit the HSP70 ATPase turnover with high percentages of inhibition: 50.42, 38.46, 50.45, 44.12, 47.13, 50.50, 40.95, 65.36, 46.23, 35.78, and 58.37 in 200 μM, respectively. Significant synergies with lapatinib were observed for compound 379 and compound 405 in the BT474 breast cancer cell line. A structure-function analysis revealed that most of the thiourea derivatives exhibited cooperative action with lapatinib in the BT474 cancer cell line and the BT/Lap^{R}1.0 lapatinib-resistant cell line. HSP70 inhibitors may be developed as synergetic drugs in drug-resistant cancer therapy.

1. Introduction

As a widely present molecular chaperone, heat-shock protein 70 (HSP70) plays important roles in the stabilization of vital proteins. HSP70 is involved in numerous cellular activities, such as the folding of newly synthesized proteins, the subcellular transport of proteins and vesicles [1], the maturation of intracellular proteins [2]and the degradation of misfolded proteins [3]. Therefore, the regulation of HSP70 enzymatic activities has become crucial to controlling cell growth and metabolic functions [4].

Although HSP70 exists in almost all living organisms, it is typically highly expressed and activated in cancer cells [5]. High levels of HSP70 in cancer cells are related with the resistance to cell death induced by heat, UV radiation, tumour necrosis factor (TNF), caspase-3 overexpression, oxidative stress, and several chemotherapeutic drugs [6–9]. At the pro-mitochondria level, HSP70 blocks the maturation of procaspase-3 and procaspase-7 to inhibit the protease-dependent apoptosis signal pathway [10]. At the mitochondrial level, HSP70 inhibits Bad and/or Bax and keeps them from translocating to the mitochondria to prevent mitochondrial outer membrane permeabilization and inhibit the release of cytochrome c, which acts upstream of mitochondrial membrane depolarization [10], and apoptosis inducing factor (AIF) to maintain the mitochondrial membrane potential [11]. At the post-mitochondrial level, it inhibits apoptosis through the release of cytochrome c and the activation of caspase-3 to prevent the recruitment of procaspase-9 to the apoptosome by directly binding to Apaf-1 [12], which prevents the formation of the active apoptosome. At the receptor level, HSP70 may promote receptor-mediated apoptosis. HSP70 mediates the Bcr-Abl-induced resistance to TNF-α-related apoptosis-inducing ligand (TRAIL)-induced apoptosis by preventing the formation of death-inducing signalling complexes involving the death receptors DR4 and DR5 [13]. In addition, HSP70 interacts with the Fanconi Anaemia Complementation Group C (FANCC) protein via its ATPase domain, and together with HSP40, it inhibits TNF-induced apoptosis through the ternary complex of HSP70, FANCC, and PKR (Fig. 1) [14,15].

It's reported that targeting the testis-specific heat-shock protein 70-2(HSP70-2) can reduces cellular growth, migration, and invasion in renal cell carcinoma cells [16]. Although the efficacy of HSP70 inhibitors as a single-agent therapy is limited due to their pharmacological and pharmacodynamic properties, they have been reported to enhance the cytotoxic activity of various antitumour

* Corresponding author.
** Corresponding author.
E-mail addresses: 21cc@163.com (R.-y. Cao), zhongwu@bmi.ac.cn (W. Zhong).

http://dx.doi.org/10.1016/j.ejmech.2016.04.042

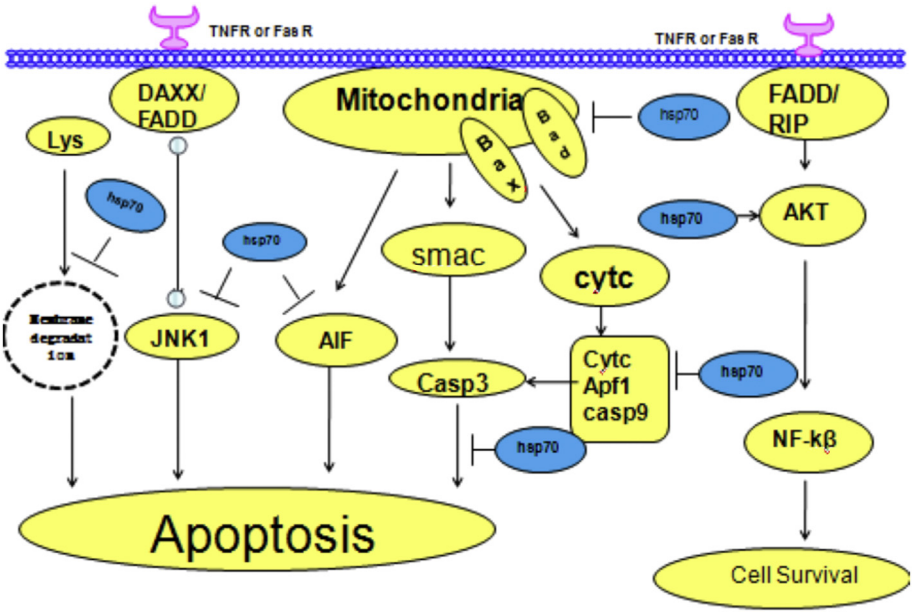

Fig. 1. Anti-cancer pathway.

agents [17]. The effect of a combination of HSP70 inhibitors with other anticancer agents in cancer therapy has been explored in recent preclinical and clinical studies, which demonstrated the synergic effects of HSP70 inhibitors in most cases [18]. Blocking the function of both heat shock protein 90 and 70 simultaneously limits these chaperones' cytoprotective effects on cancer cells. And the unique phenotype associated with modulating Hsp90's C-terminus, a synergistic and highly relevant dual chemotherapy regimen was produced when it used in combination with Hsp70 inhibitors [19]. The inhibition of HSP70 in cancer cells may reduce the incidence of drug resistance. In this study, we aimed to design a series of novel HSP70 inhibitors that exert synergic effects with anticancer agents.

2. Computational methods

All members of the Hsp70 family have an N-terminal nucleotide binding domain (NBD) (~40 kDa) and a C-terminal substrate-binding domain (SBD) (~25 kDa) connected by a short linker (Fig. 2). The X-ray structure of HSP70 NBD in complex with ADP (PDB ID: 3I33) from the Brookhaven Protein Data Bank (http://www.rscb.org/pbd/) was used for virtual screening using the DOCK4.0 software. The database originated from ACD and our patented compound library. The target protein was prepared using the Chimera software. The grid-based energy scoring function was used to evaluate the affinity of the designed inhibitors to HSP70. The energy scoring component of DOCK 4.0 was based on the implementation of force field scoring. Force field scores are approximate molecular mechanics interaction energies consisting of van der Waals and electrostatic components: $\Delta G_{binding} \approx \Delta H_{binding}$. An anchor-first search was used for the small-molecule-conformation search. The optimized fragments were selected by critical site point matching, chemical matching and energy minimization. Ultimately, the top 1000 molecules were selected. More extensive docking was performed using MVD (Molecular Virtual Docker, Version 2010.4.0) with ADP as the ligand template. Hydrogen bonds were formed between ADP and the amino acid residues Thr15, Tyr16, Gly205, Glu271, Lys274, Ser278, Gly342, and Arg345 (Fig. 3). The energy grid used a 0.4-Å resolution. The MolDock score [Grid] was chosen as the scoring function with 0.3-Å resolution. Based on the current resolution and the search space size, the grid requires approximately 46.7 MB of memory. The number of maximal iterations, maximal population size, and the numbers of pose generations, simplex evaluations, and docking runs were set to 1500, 50, 100, 300, and 10, respectively.

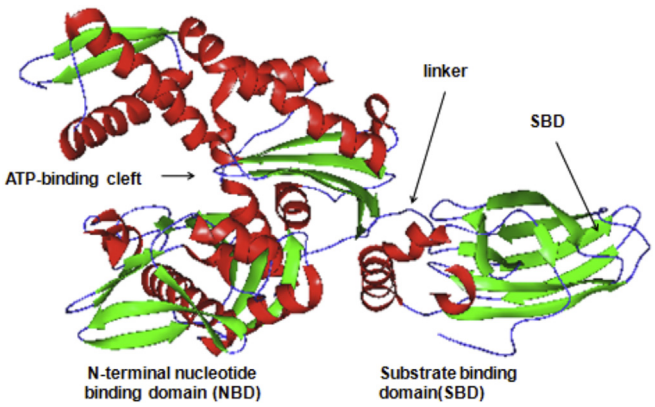

Fig. 2. Three-dimensional structure of HSP70.

Several structural units were selected. Among them, the N, N′-disubstituted thiourea derivatives (Fig. 4) from our patented compound library (Patent CN103387551A) were the most attractive due to their perfect binding results. For example, hydrogen bonds were formed between compound PP1-051 (Fig. 3) and the amino acid residues Thr14, Thr15, Gly205, Gly206 and Thr207. The binding profiles of some of the compounds to HSP70 were almost similar to that found for ADP.

This series of compounds from our patented compound library have been reported to be used for the protection of cells from apoptosis induced by endoplasmic reticulum (ER) stress [20]. Moreover, it has been revealed that the trichloromethyl group greatly contributes to the activity. Therefore, we designed and prepared novel N, N′-disubstituted thiourea derivatives as HSP70 inhibitors by changing the R_3 from CX_3 to a short-chain fatty acid to establish a peptidomimetic effect (Fig. 5).

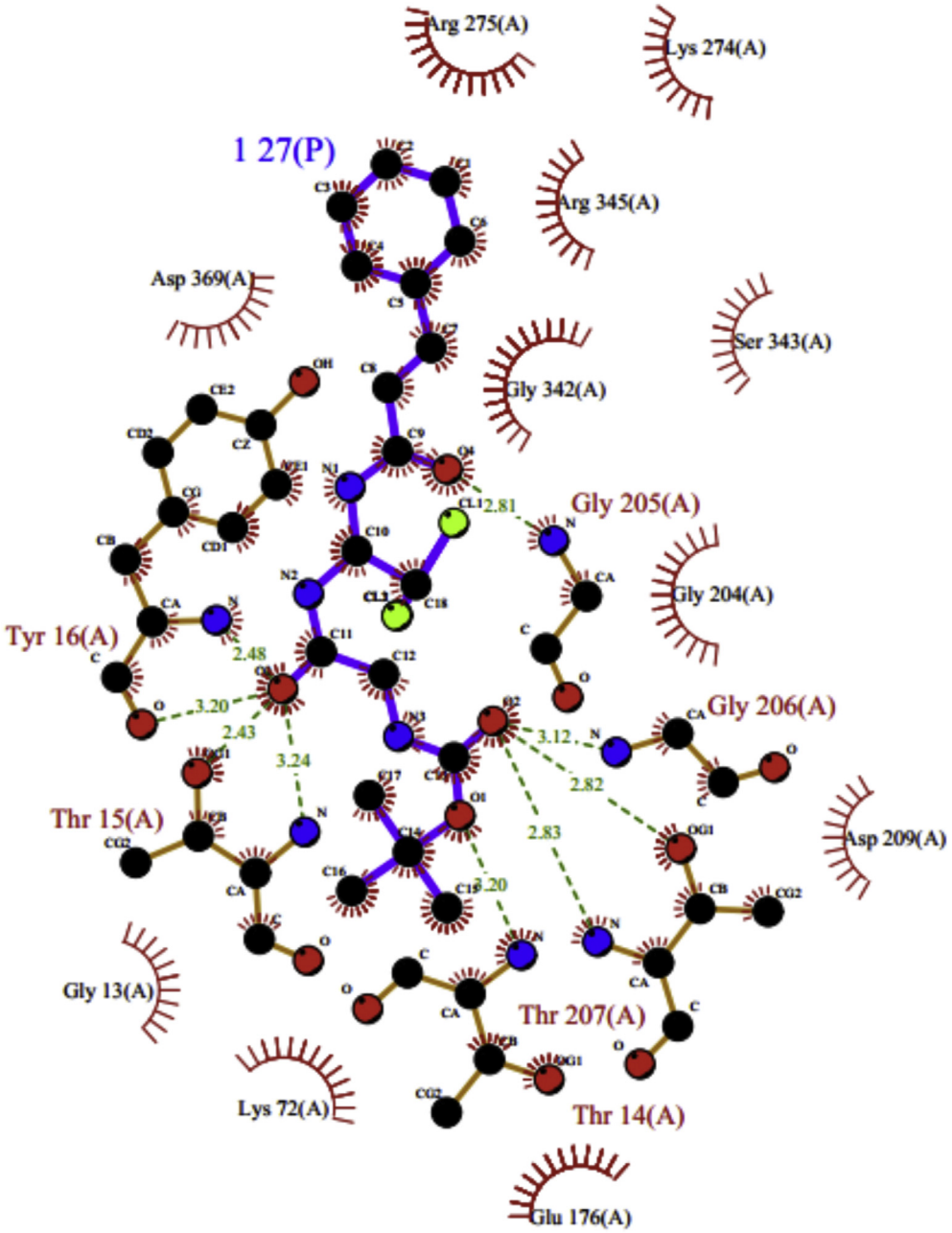

Fig. 3. Schematic of the residues that interact with PP1-051. The figure was produced using the LigPlus program. Hydrogen bonds are indicated by dashed lines between the atoms involved, whereas hydrophobic contacts are represented by an arc with spokes radiating toward the contact site. The contact atoms are shown with spokes radiating back. The HSP70 residues are identified by the three-letter amino acid codes. Colour coding: ligand residue names, blue; hydrophobic residue names, black; ligand bonds, purple; non-ligand bonds, orange; hydrogen bonds, olive green; and hydrophobic "bonds", brick red. (For interpretation of the references to colour in this figure legend, the reader is referred to the web version of this article.)

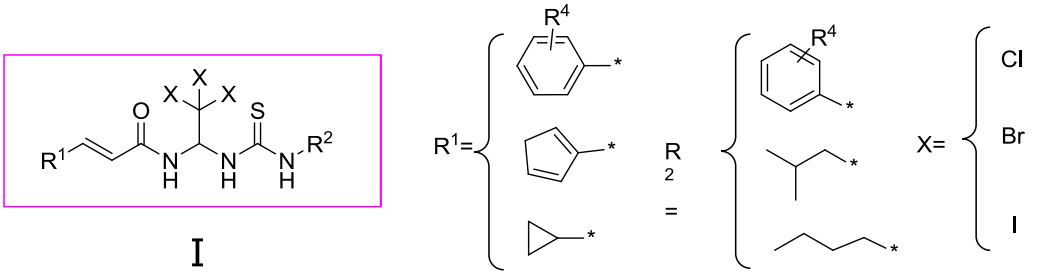

Fig. 4. Screened nuclear structure from our database.

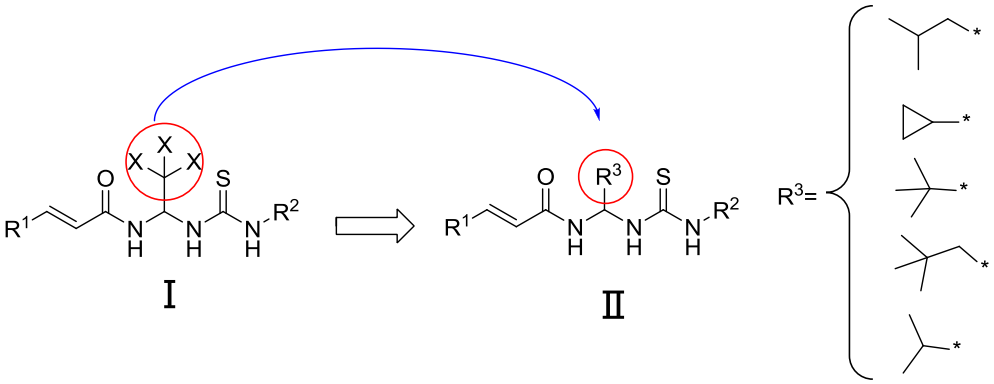

Fig. 5. CX_3 was changed to a short-chain fatty acid.

The modelled structures of the newly designed molecules were computationally docked into the crystal structure of the HSP70 NBD. Docking was accomplished using a previously described protocol based on the Sybyl6.9 software and the scoring function grid score. As shown in Fig. 6A and B, the docking results of compound 371 and compound 375 revealed several key amino acid residues in the binding pocket, such as Thr15, Arg275 and Asp369.

3. Results and discussion

3.1. Chemistry

The compounds 370–409 were synthesized as shown in Scheme 1. The reaction of a commercially available aldehyde (1) with malonic acid yielded an α, β-unsaturated acid (2) via an aldol condensation reaction, and this compound was then reacted with 4-methylbenzoyl chloride to yield the product (3). Substituted α, β-unsaturated amides (4) were obtained via an aminolysis reaction of product (3) with concentrated ammonia in chloroform. The reaction of α, β-unsaturated amides (4) with the fatty aldehyde and benzotriazole in the presence of p-toluenesulphonic acid produced benzotriazole intermediates (5) [21], which were coupled with amines (8) to yield the desired products, as shown in Table 1. The intermediate (8) was acquired by the treatment of product (7) with concentrated ammonia in methanol. The reaction of ammonia with carbon disulphide and methyl iodide in DMSO yielded intermediate (7).

3.2. Colorimetric determination of HSP70 ATPase activity

In the preliminary screening system, the compounds that were found to inhibit HSP70 ATPase activity by 20% at the concentration of 200 μM were defined as effective inhibitors [22,23]. Two positive control compounds were applied to verify the accuracy of the screening system. The inhibition rate of the control compounds AZ [23] and VER155008 [22] reached 53.13% and 43.03%, respectively, indicating the high efficacy and accuracy of the experimental system.

Dose-dependent effects were observed for AZ and VER155008 (positive control) when these were incubated at multiple concentrations (200 μM, 100 μM, 50 μM, 25 μM, and 12.5 μM) with HSP70 (Fig. 7). The compounds 370/371/374/379/380/392/394/397/404/405 and 407 were identified as potential inhibitors because their inhibition rates were greater than 20% in multiple experiments (Table 2, Fig. 8).

3.3. Resistance reversal test to lapatinib

All of the compounds were tested to determine their drug resistance reversal effect to lapatinib *in vitro*. The luminescent signal indicating the ATP level was measured, and the data were normalized to that obtained for the control group. The cell viability was determined by the luminescence: cell viability (%) = $RLU_{experimental\ group}/RLU_{blank\ control\ group} \times 100\%$. Simultaneously, the coefficient of drug interaction (CDI) [24,25] was used for the quantification of the drug-interaction properties: CDI = AB/(A × B) × 100%, based on the cell viability. A synergetic effect was defined as CDI < 1, and a significant synergetic effect was defined as CDI < 0.7. The inhibition rates of the thiourea derivatives 370–409 for BT474 breast cancer cells and BT/Lap^R1.0 lapatinib-resistant cells are shown in Table 3. No inhibition of BT474 and BT/Lap^R1.0 was observed when the HSP70 inhibitors were administered

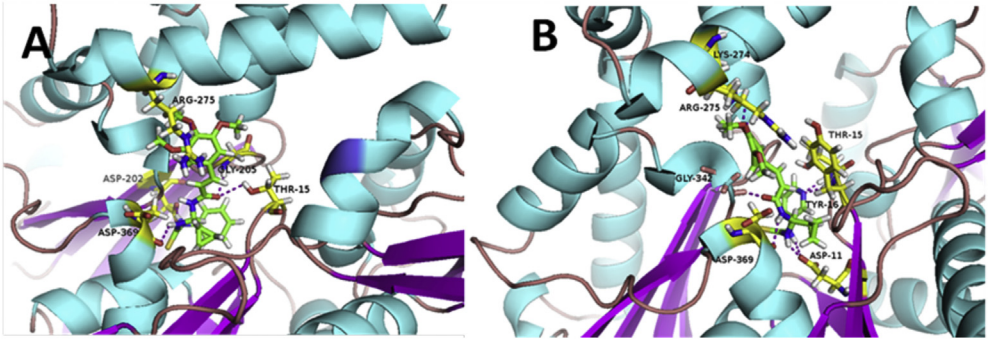

Fig. 6. Docking-predicted binging poses of compound 371 (Fig. 6A) and compound 375 (Fig. 6B). The interactions were analysed through computational docking, and the diagrams were created using the PyMol software.

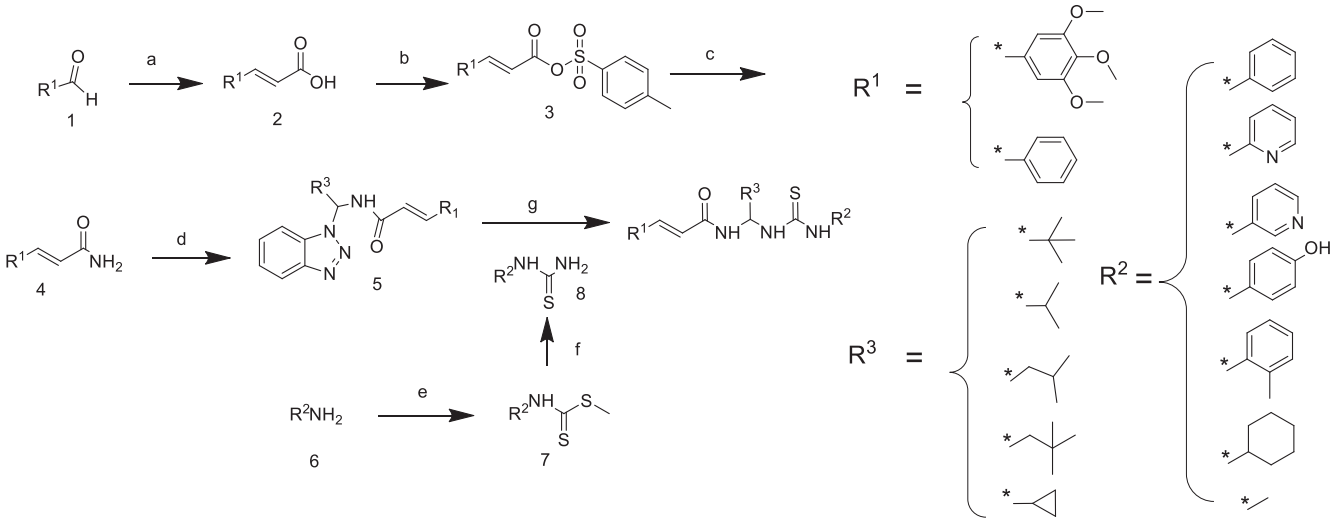

Scheme 1. Synthetic pathways for N, N′-disubstituted thiourea derivatives 370–409. Reagents and conditions: a: malonic acid, pyridine, piperidine, reflux, 6 h; b: p-toluenesulphonyl chloride, Cl_2CH_2, tetramethylammonium bromide (TMAB), K_2CO_3; c: $NH_3 \cdot H_2O$, DAEI, DCM; d: (1) benzotriazole, R^3CHO, toluene, reflux, 12 h; e: (1) R^2NH_2, CS_2, DMSO, 60 °C, 6 h; (2) ICH_3, rt, 10 h; f: $NH_3 \cdot H_2O$, MeOH, reflux, 2 h; g: NaH, THF, rt, 1 h.

independently (Table 3), but significant synergies were observed when compound 379 and compound 405 were administered together with lapatinib with CDI values of 0.65 and 0.56, respectively (Table 4, Fig. 9A and D). Synergies effects were also observed for the compounds 393/394/406 in BT/Lap^{R}1.0 cells (Table 5). Most of the thiourea derivatives showed cooperative action with lapatinib in BT474 and BT/Lap^{R}1.0 cells (CDI < 1) (Figs. 10 and 11).

4. Conclusions

In this study, synergistic effects with an anti-cancer agent were verified *in vitro* for N, N′-disubstituted thiourea derivatives, which may reduce the dose of the anti-cancer agent, thereby abating its toxicity or drug resistance during cancer treatment. Compound 379 and compound 405 presented significant synergy with lapatinib in the BT474 cell line with CDI values of 0.65 and 0.56, respectively (Table 4). The compounds 393/394/406 showed a minor synergistic effect in BT/Lap^{R}1.0 cells. Therefore, some of the novel HSP70 inhibitors were found to have obvious clinical significance. In addition, the inhibition activities of the compounds 370/371/374/379//380/392/394/397/404/405 and 407 were demonstrated through *in vitro* zymological experiments, and these results suggested that the synergetic effects are related to the inhibition of HSP70 activity. However, the underlying mechanism remains to be elucidated.

X-ray crystal structures of HSP70 (3I33) were used for the design and docking of the HSP70 inhibitors; thus, more detailed information on the relationship between the inhibitor structures and functions was obtained. This information may be important for the development of effective HSP70 inhibitors. Through the determination of their therapeutic synergism and HSP70 ATPase activity, we can better explore how those compounds enhance the therapeutic effect of anti-tumour agents via interacting with HSP70 and thus develop more favourable drugs.

5. Materials and methods

5.1. Chemistry

The ^{1}H NMR spectra were recorded in DMSO-d_6 using a Bruker-ARX400 spectrometer with TMS as the internal standard. All chemical shifts are presented in δ values (ppm). The MS spectra were recorded using a Micromass ZabSpect. Elemental analyses were performed with an Elementar Vario MICRO CUBE (Germany).

5.2. Compounds

5.2.1. Synthesis of N, N′-disubstituted thiourea derivatives 370-409

General procedures: Aromatic formaldehyde (10 mmol) and malonic acid (30 mmol) were stirred in dry pyridine (20 mL) for 8 h with one drop of piperidine as the catalyst. The mixture was poured into 20 mL of water, and 10% NaOH (aq) was used to adjust the pH to 12. After three extractions with ethyl acetate, 2 N HCl (aq) was added to the water layer until a white precipitate (2) appeared in 85% yield.

Intermediate 2: (E)-3-(3, 4, 5-trimethoxyphenyl)acrylic acid. ^{1}H NMR (400 MHz, $CDCl_3$-*d*)δ3.90 (s, 9H); δ6.35–6.39 (d, 1H, J = 16 Hz); δ6.79 (s, 2H); δ7.69–7.73 (d, 1H, J = 16 Hz).

The white precipitate (2, 20 mmol) was dissolved in dry DCM (30 mL). p-Toluenesulphonyl chloride (22 mmol), tetramethylammonium bromide (10 mmol) and K_2CO_3 (20 mmol) were added, and the mixture was refluxed for 40 min. The solvent was removed under reduced pressure. Ten millilitres of methanol was added to the resulting residue, and the mixture was stirred for 5 min. The white solid (3) that precipitated from the solution was collected by filtration and washed with methanol. The white solid (15 mmol) and DIEA (20 mmol) in DCM (20 mL) were stirred, and $NH_3 \cdot H_2O$ (40 mmol) was added. The mixture was then refluxed at 6 h. Saturated sodium bicarbonate solution (20 mL) was added to the solution and extracted with DCM (20 mL × 5). The organic phase was collected, washed with brine (20 mL × 3), dried over Na_2SO_4 and concentrated under reduced pressure to obtain the desired product (4) in 80% yield.

Intermediate 4: (E)-3-(3, 4, 5-trimethoxyphenyl)acrylamide. ^{1}H NMR (400 MHz, $CDCl_3$-*d*)δ3.89 (s, 9H); δ5.66 (s, 2H); δ6.36–6.40 (d, 1H, J = 15.6 Hz); δ6.75 (s, 2H); δ7.55–7.59 (d, 1H, J = 15.6 Hz). MS238.2 $[M+H]^+$.

A suspension of the product (4, 8 mmol), the corresponding aldehyde (16 mmol) and benzotriazole (24 mmol) in toluene (30 mL) was treated with concentrated HCl (nine drops). The solution was heated at reflux under Dean–Stark conditions for 20 h, cooled to ambient temperature, and concentrated under reduced pressure. Twenty millilitres of methanol was added, and the

Table 1
Structures of N, N′-disubstituted thiourea derivatives 370–409[a].

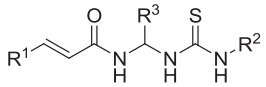

ID	R^1	R^2	R^3	Melting point (°C)	ID	R^1	R^2	R^3	Melting points (°C)
370				105–108	389				174–176
371				159–162	390				166–168
372				175–178	391				90–92
373				173–174	392				206–208
374				148–150	393				H-393
375				168–170	394				168–170
376				222–224	395				119–121
378				115–117	396				182–184
379				168–169	397				188–190
380				115–117	402				97–100
381				186–189	404				180–182
382				216–219	405				182–184
383				146–150	406				166–168
384				195–198	407				138–141
386				152–155	408				174–176
387				120–122	409				192–194
388				178–180					

[a] All of those compounds are white solid.

mixture was stirred for 5 min. The white precipitate that was formed was collected by filtration and washed with 50% ether/hexanes (20 mL) to provide the desired product (5) as a white solid in 45%–60% yield.

Intermediate 5: (E)-N-(1-(1H-benzo[d] [1,2,3]triazol-1-yl)-2,2-dimethylpropyl)-3-(3,4,5-trimethoxyphenyl)acrylamide: MS 425.5 $[M+H]^+$. (E)-N-(1-(1H-benzo[d] [1,2,3]triazol-1-yl)-3-methylbutyl)-3-(3,4,5-trimethoxyphenyl)acrylamide: MS425.5 $[M+H]^+$. N-(1-(1H-benzo[d] [1,2,3]triazol-1-yl)-3,3-dimethylbutyl) cinnamamide: MS349.5 $[M+H]^+$. N-(1-(1H-benzo[d] [1,2,3]triazol-1-yl)-3-methylbutyl)cinnamamide: MS335.2 $[M+H]^+$. N-(1-(1H-benzo[d] [1,2,3]triazol-1-yl)-2,2-dimethylpropyl)cinnamamide: MS 335.3 $[M+H]^+$.

DMSO (15 mL) and KOH (11 mmol) were added to a round-bottomed flask and cooled to 0 °C. To this solution, carbon disulphide (15 mmol) was added, and the mixture was stirred for

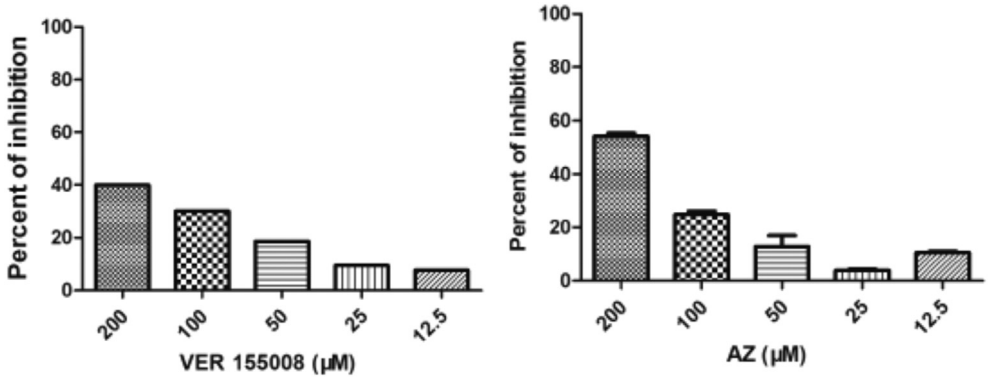

Fig. 7. Percentage of inhibition of HSP70 ATPase activity achieved by the positive controls VER 155008 and AZ at different concentrations.

Table 2
Inhibition of HSP70 ATPase activity by the tested compounds at a concentration of 200 μM.

ID	Percent inhibition (%)	SD
AZ	53.04	0.89
VER155008	43.03	3.01
370	50.42	3.92
371	38.46	5.65
374	50.45	13.04
379	44.12	1.95
380	47.13	1.72
392	50.50	1.01
394	40.95	5.00
397	65.36	8.30
404	46.23	5.81
405	35.78	14.98
407	58.37	9.22

10 min. The amine (10 mmol) in DMSO (5 mL) was then added dropwise for 20–30 min with constant stirring, and the mixture was then heated to 60 °C for 6 h and cooled to room temperature. After ICH_3 (20 mmol) was added, the mixture was stirred at room temperature for 10 h. Water (50 mL) was added to the solution and extracted with DCM (30 mL × 3). The organic phase was collected, washed with brine (20 mL × 3), dried over Na_2SO_4 and concentrated under reduced pressure to obtain the desired product (7) in 55%–82% yield.

Intermediate 7: methyl phenylcarbamodithioate. ^{1}H NMR (400 MHz, $CDCl_3$-*d*) δ2.69 (s, 3H); δ7.10–7.13 (t, 2H); δ7.30–7.34 (t, 2H); δ7.38–7.40 (d, 1H); δ9.69 (s, 1H). Methyl pyridin-3-ylcarbamodithioate: ^{1}H NMR (400 MHz, DMSO-d_6) δ2.69 (s, 3H); δ7.38–7.42 (t, 2H, J = 8.12 Hz and 4.76 Hz); δ8.22 (s, 1H); δ8.52–8.53 (dd, 1H, J = 4.76 Hz and 1.12 Hz); δ8.71–8.72 (d, 1H, J = 2.52 Hz); δ9.03 (s, 1H).

A solution of 8 (5 mmol) in methanol (10 mL) was treated with concentrated ammonia (10 mmol). The mixture was heated at reflux for 2 h, concentrated under reduced pressure, and extracted with DCM and water (three times), and the organic phase was then collected, washed with brine (20 mL × 3), dried over Na_2SO_4 and concentrated under reduced pressure to obtain the desired product (8) in 80%–90% yield.

Intermediate 8: Phenylthiourea. ^{1}H NMR (400 MHz, $CDCl_3$-*d*) δ7.10–7.13 (t, 2H); δ7.30–7.34 (t, 2H); δ7.38–7.40 (d, 1H); δ9.69 (s, 1H). MS153.0 $[M+H]^+$. 1-(pyridin-3-yl)thiourea: ^{1}H NMR (400 MHz, DMSO-d_6)δ7.34–7.37 (dd, 2H, J = 8.44 Hz and 4.76 Hz);

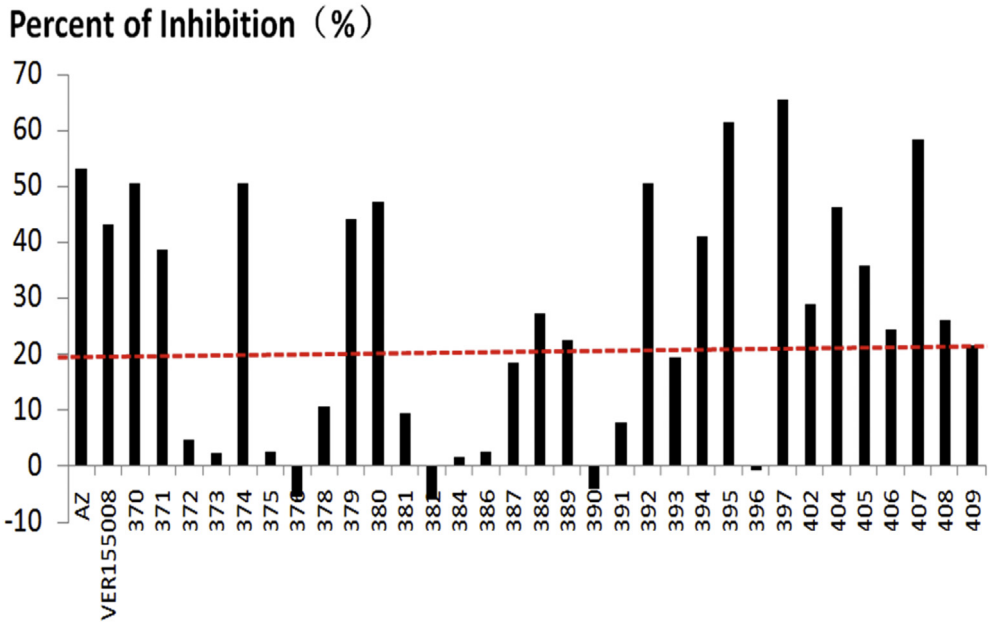

Fig. 8. Percentage of inhibition of HSP70 ATPase activity achieved by the test compounds at a concentration of 200 μM.

Table 3
Inhibition of the breast cancer cells BT474 and BT/Lap^{R}1.0 by the N, N′-disubstituted thiourea derivatives 370–409.

ID	Inhibition (%) of BT474		Inhibition (%) of BT/Lap^{R}1.0	
	10 μM	10 μM + 1 μM lapatinib	10 μM	10 μM + 1 μM lapatinib
370	7.3	76.6	9.4	42.2
371	9.2	79.1	10.5	54.2
372	2.2	83.2	2.9	48.8
373	10.3	84.7	16	56
374	12.2	85.2	13.7	56
375	8.6	85.2	12.3	55.7
376	20.1	87.8	17.4	59.6
378	24.9	87.8	38.7	61
379	19	90.9	40.9	62.3
380	22.1	89.9	19.3	59.9
381	25.8	88.5	31.5	65.9
382	12.4	86.2	18.2	57.6
383	4.8	79.1	11.4	32.8
384	2.4	78.8	6	25.2
386	17.7	85	13.6	36.9
387	11.3	84.9	34.6	53
388	9.6	83.5	11.4	33
389	3.8	81.4	8.7	27.8
390	9.4	82	11.5	30
391	10.5	79.8	13	30.9
392	8.2	81.4	9.9	30.1
393	44	87.4	6.8	44.2
394	18.2	84.2	18.9	41
395	9.8	81.6	12.8	23.3
396	7	78.7	9.7	20.5
397	6	78.6	8.7	20
402	11.5	78.5	15.4	23.4
404	16.5	83.4	38.8	48.1
405	13.5	87.3	39.8	57.8
406	15.3	82.2	22.6	45.7
407	13.5	84	19.8	33.4
408	10.3	80.6	13.3	75.8
409	13	85.2	34.3	47.2

Note: The administration of lapatinib at a concentration of 1 μM resulted in inhibition percentages of 75.6% and 18% on the breast cancer cells BT474 and BT/Lap^{R}1.0, respectively.

Table 4
CDI values of N, N′-disubstituted thiourea derivatives for BT474 cells.

ID	BT474 (CDI)	ID	BT474 (CDI)
379	0.65	395	0.84
380	0.81	404	0.73
386	0.86	405	0.56
387	0.79	406	0.82
388	0.85	407	0.77
394	0.74	409	0.77

δ7.93–7.95 (d, 1H, J = 8.12 Hz); δ8.30–8.31 (dd, 1H, J = 4.52 Hz and 1.12 Hz); δ8.54–8.55 (d, 1H, J = 2.8 Hz); δ9.79 (s, 1H). MS154.0 $[M+H]^+$. 1-(pyridin-2-yl)thiourea: ^{1}H NMR (400 MHz, $CDCl_3$-*d*) δ6.9–6.92 (d, 1H, J = 8.16 Hz); δ7.00–7.03 (q, 1H); δ7.11 (s, 1H); δ7.66–7.70 (m, 1H); δ8.22–8.23 (dd, 1H, J = 5.08Hzv); δ9.15 (s, 1H); δ11.10 (s, 1H). MS154.0 $[M+H]^+$. 1-(4-methoxyphenyl)thiourea: MS182.8 $[M+H]^+$.

Compounds 8 (2 mmol) and 5 (2 mmol) in THF (5 mL) were added to NaH (2.4 mmol) in one portion. The mixture was stirred at room temperature for 1 h, extracted three times with ethyl acetate, washed twice with saturated sodium chloride, dried over anhydrous sodium sulphate, and concentrated to yield a residue that was chromatographed (ethyl acetate:petroleum ether = 1:1) to the pure product 370–409 in 55%–76% yield.

5.2.1.1. (E)-N-(3-methyl-1-(3-phenylthioureido)butyl)-3-(3,4,5-trimethoxyphenyl) acrylamide (370). ^{1}H NMR (400 MHz, DMSO-d_6) δ0.90–0.94 (m, 6H); δ1.48–1.71 (m, 4H); δ3.68 (s, 3H); δ3.80 (s, 6H); δ6.48–6.52 (d, 2H); δ6.86 (s, 2H); δ7.02 (s, 1H); δ7.38–7.48 (m, 4H); δ8.08 (s, 1H). ^{13}CNMR (DMSO, 100 MHz) δ21.88; 24.40; 42.88; 55.86; 59.56; 60.12; 105.04; 119.68; 121.40; 122.95; 124.21; 128.53; 130.29; 138.76; 139.29; 139.40; 153.10; 164.75; 179.39. MS 458.4 $[M+H]^+$.

5.2.1.2. (E)-N-(3-methyl-1-(3-pyridin-3-ylthioureido)butyl)-3-(3,4,5-trimethoxyphenyl) acrylamide (371). ^{1}H NMR (400 MHz, CCl_3D-d_6) δ0.94 (s, 6H); δ1.71–1.48 (m, 3H); δ3.80 (m, 1H); δ3.87–3.89 (s, 10H); δ5.66 (s, 1H); δ6.39–6.43 (d, 1H, J = 15.68 Hz); δ6.75 (s, 2H); δ6.92–6.94 (d, 1H, J = 6.2 Hz); δ7.04–7.07 (d, 1H, J = 8.96 Hz); δ7.30–7.33 (q, 1H, J = 8.4 Hz and 4.76 Hz); δ7.65–7.67 (d, 1H, J = 15.68 Hz); δ8.21–8.23 (d, 1H, J = 7 Hz); δ8.41–8.43 (dd, 1H, J = 6.2 Hz and 1.44 Hz); δ8.82 (s, 1H); δ10.95 (s, 1H). ^{13}C NMR (CD_3OD, 100 MHz) δ21.96; 25.49; 42.86; 43.24; 56.11; 58.46; 60.65; 105.90; 118.29; 124.25; 131.34; 132.73; 138.28; 143.43; 145.15; 145.32; 154.24; 169.18; 182.02. MS 459.6 $[M+H]^+$.

5.2.1.3. (E)-N-(2,2-dimethyl-1-(3-phenylthioureido)propyl)-3-(3,4,5-trimethoxyphenyl) acrylamide (372). ^{1}H NMR (400 MHz, DMSO-d_6) δ0.87–0.96 (m, 9H); δ3.68 (s, 3H); δ3.80 (s, 6H); δ6.14 (s, 1H); δ6.60–6.62 (d, 1H); δ6.91 (s, 2H); δ7.12–7.13 (t, 1H); δ7.31–7.35 (t, 3H); δ7.52–7.54 (d, 2H); δ7.62 (d, 1H); δ8.11 (s, 1H); δ9.85 (s, 1H). ^{13}CNMR (CD_3OH, 100 MHz) δ21.88; 24.40; 42.88; 56.13; 60.67; 105.04; 120.35; 121.40; 122.95; 124.21; 128.53; 131.55; 138.76; 140.25; 140.19; 154.26; 170.41; 180.09. MS 458.6 $[M+H]^+$.

5.2.1.4. (E)-N-(2,2-dimethyl-1-(3-pyridin-3-ylthioureido)propyl)-3-(3,4,5-trimethoxyphenyl)acrylamide (373). ^{1}H NMR (400 MHz, CCl_3D-*d*) δ0.90–1.15 (s, 9H); δ3.84–3.90 (s, 9H); δ5.42 (m, 1H); δ6.44–6.46 (m, 1H); δ6.49–6.53 (d, 1H); δ6.64–6.66 (d, 1H); δ6.78 (s, 2H); δ7.29–7.32 (q, 1H, J = 8.2 Hz, J = 4.76 Hz); δ7.69–7.73 (d, 1H, J = 7.84 Hz); δ8.26–8.42 (d, 1H, J = 7.84 Hz); δ8.42–8.43 (dd, 1H, J = 4.76 Hz, J = 1.4 Hz); δ8.74–8.75 (d, 1H, J = 1.96 Hz; δ10.55 (s, 1H). ^{13}C NMR (DMSO, 100 MHz) δ25.45; 55.81; 59.98; 66.16; 104.97; 121.40; 122.91; 130.04; 130.42; 136.49; 138.72; 139.23; 144.25; 144.71; 152.98; 164.18; 181.11. MS 459.4 $[M+H]^+$.

5.2.1.5. (E)-N-(cyclopropyl(3-phenylthioureido)methyl)-3-(3,4,5-trimethoxy-phenyl)acrylamide (374). ^{1}H NMR (400 MHz, DMSO-d_6) δ0.91 (m, 1H); δ2.05–2.07 (m, 2H); δ3.75 (s, 4H); δ3.79–3.80 (m, 2H); δ3.88 (s, 6H); δ6.03 (m, 1H); δ6.71–6.75 (d, 1H); δ7.03 (s, 2H); δ7.16–7.22 (m, 1H); δ7.36–7.40 (t, 2H); δ7.59–7.61 (d, 2H); δ9.24 (s, 1H); δ10.60 (s, 1H). ^{13}CNMR (DMSO, 100 MHz) δ15.26; 55.84; 60.02; 62.93; 105.10; 120.90; 122.95; 124.13; 128.34; 128.47; 130.26; 138.87; 139.34; 153.02; 164.71; 179.39. MS 442.4 $[M+H]^+$.

5.2.1.6. (E)-N-(cyclopropyl(3-pyridin-3-ylthioureido)methyl)-3-(3,4,5-trimethoxyphenyl) acrylamide (375). ^{1}H NMR (400 MHz, CCl_3D-*d*) δ0.51–0.57 (m, 4H); δ1.25–1.26 (m, 1H); δ2.45 (s, 1H); δ3.87 (s, 9H); δ4.99 (s, 1H); δ6.43–6.47 (d, 1H); δ6.74 (s, 1H); δ7.27–7.31 (m, 2H); δ7.41–7.43 (d, 1H, J = 8.4 Hz); δ7.63–7.67 (d, 1H); δ8.18 (s, 2H); δ8.39–8.40 (d, 1H); δ8.79 (s, 1H); δ10.78 (s, 1H). ^{13}C NMR (DMSO, 100 MHz) δ15.57; 56.15; 60.42; 63.35; 105.32; 121.55; 123.40; 130.65; 136.50; 139.06; 139.65; 144.78; 145.27; 153.38; 164.33; 180.27. MS 443.5 $[M+H]^+$.

5.2.1.7. (E)-N-(cyclopropyl(3-pyridin-2-ylthioureido)methyl)-3-(3,4,5-trimethoxyphenyl) acrylamide (376). ^{1}H NMR (400 MHz, DMSO-d_6) δ0.45–0.50 (m, 4H); δ1.45–1.47 (m, 1H); δ3.68 (s, 3H); δ3.81 (s, 6H); δ5.92–5.94 (m, 1H); δ6.55–6.59 (d, 1H, J = 15.68 Hz); δ6.91 (s, 1H); δ7.06–7.09 (m, 1H); δ7.17–7.19 (d, 1H, J = 8.4 Hz); δ7.37–7.41 (d, 1H, J = 15.68 Hz); δ7.79–7.80 (m, 1H); δ8.24–8.26 (d, 1H, J = 1.4 Hz and 5.04 Hz)δ8.61–8.63 (d, 1H, J = 7.84 Hz); δ10.66 (s, 1H); δ12.17–12.19 (d, 1H, J = 8.12 Hz). ^{13}C NMR (DMSO, 100 MHz)

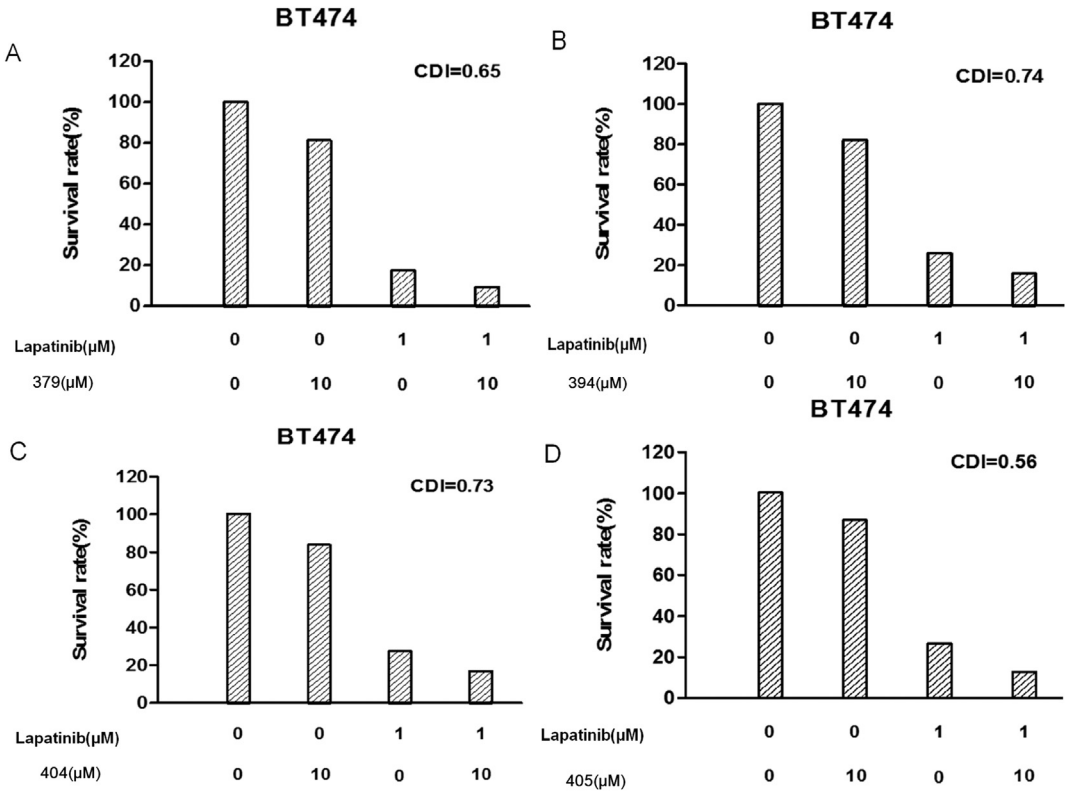

Fig. 9. CDI values of the compounds 379, 394, 404 and 405 for BT474 cells.

Table 5
CDI values of N, N′-disubstituted thiourea derivatives for BT/Lap^{R}1.0 cells.

ID	BT/Lap^{R}1.0 (CDI)	ID	BT/Lap^{R}1.0 (CDI)
393	0.79	405	0.86
394	0.79	406	0.8

δ1.60; 2.07; 15.41; 55.84; 60.11; 63.09; 104.93; 112.74; 118.06; 121.29; 130.46; 138.65; 139.15; 139.55; 145.64; 153.07; 153.68; 164.29; 178.93. MS 443.3 $[M+H]^+$.

5.2.1.8. (E)-N-(3-methyl-1-(3-pyridin-2-ylthioureido)butyl)-3-(3,4,5-trimethoxyphenyl)acrylamide (378). ^{1}H NMR (400 MHz, CCl_3D-*d*) δ1.00–1.01 (s, 6H); δ1.73–1.76 (m, 2H); δ2.16 (s, 2H); δ3.87 (s, 9H); δ5.88 (s, 1H); δ6.32–6.36 (d, 1H, J = 15.74 Hz); δ6.71–6.76 (m, 3H); δ6.98–7.00 (m, 1H); δ7.09 (m, 1H); δ7.51–7.55 (d, 1H, J = 15.74 Hz); δ7.64 (m, 1H); δ8.24–8.25 (m, 1H); δ10.32 (s, 1H). ^{13}CNMR (DMSO, 100 MHz) δ21.84; 22.96; 24.54; 42.94; 55.84; 60.09; 104.94; 112.64; 117.94; 121.24; 130.37; 138.67; 139.05; 139.58; 145.59; 153.07; 153.72; 164.53; 178.32. MS 459.2 $[M+H]^+$.

5.2.1.9. (E)-N-(3,3-dimethyl-1-(3-phenylthioureido)butyl)-3-(3,4,5-trimethoxyphenyl)acrylamide (379). ^{1}H NMR (400 MHz, DMSO-d_6) δ0.95 (s, 9H); δ1.79 (s, 2H); δ3.69 (s, 3H); δ3.82 (s, 6H); δ6.08 (m, 1H); δ6.57–6.60 (d, 1H); δ6.92 (s, 2H); δ7.12–7.14 (m, 1H); δ7.31–7.49 (m, 5H); δ7.94 (s, 1H); δ8.57 (s, 1H); δ9.72 (s, 1H). ^{13}C NMR (DMSO, 100 MHz) δ179.42; 164.98; 153.60; 139.92; 139.30; 130.93; 129.09; 124.75; 123.45; 122.06; 105.49; 60.62; 59.69; 56.35; 48.11; 30.24. MS 472.3 $[M+H]^+$. The results of 2D ^{13}C, ^{1}H

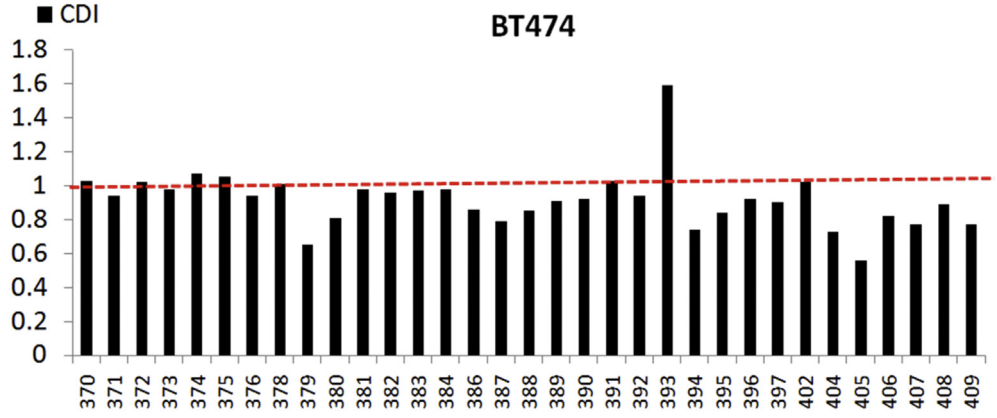

Fig. 10. Coefficient of drug interaction (CDI) of thiourea derivatives with lapatinib *in vitro* toward BT474 cells.

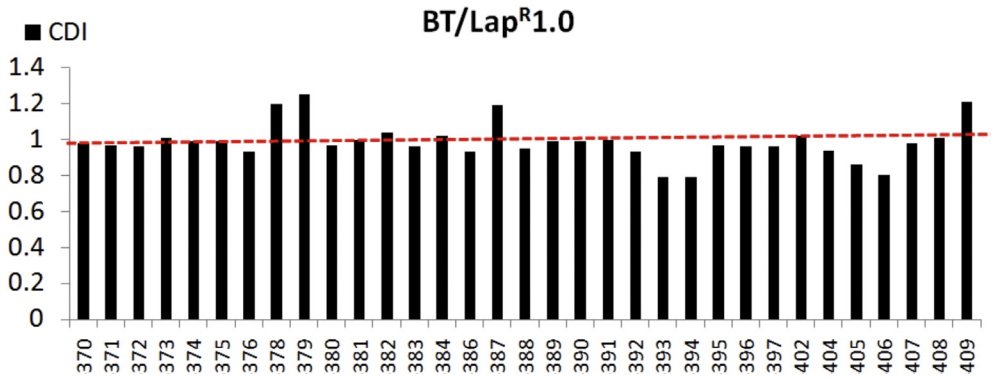

Fig. 11. Coefficient of drug interaction (CDI) of thiourea derivatives with lapatinib *in vitro* toward BT/Lap^{R}1.0 cells.

COSY(HMQC) spectra of compound 379 was shown in Table 6.

5.2.1.10. (E)-N-(3,3-dimethyl-1-(3-pyridin-3-ylthioureido)butyl)-3-(3,4,5-trimethoxyphenyl)acrylamide (380). ^{1}H NMR (400 MHz, CCl_3D-*d*) δ1.01 (s, 9H); δ1.79–1.82 (m, 1H); δ2.05 (m, 2H); δ3.89 (s, 9H); δ5.71 (s, 1H); δ6.37–6.41 (d, 1H, J = 15.44 Hz); δ6.76 (m, 2H); δ7.02–7.04 (d, 1H, J = 7.28 Hz); δ7.31–7.34 (m, 1H); δ7.67–7.71 (d, 1H, J = 15.44 Hz); δ8.24–8.26 (d, 1H, J = 6.16 Hz); δ8.42–8.43 (d, 1H); δ8.83 (s, 1H); δ10.92 (s, 1H). ^{13}C NMR (DMSO, 100 MHz) δ29.49; 29.74; 29.99; 55.71; 55.88; 60.13; 104.92; 105.23; 121.88; 123.35; 130.35; 136.28; 139.42; 144.25; 144.99; 153.11; 164.53; 179.54. MS 473.3 $[M+H]^+$.

5.2.1.11. (E)-N-(3,3-dimethyl-1-(3-pyridin-2-ylthioureido)butyl)-3-(3,4,5-trimethoxyphenyl)acrylamide (381). ^{1}H NMR (400 MHz, CCl_3D-*d*) δ1.02 (s, 9H); δ1.74 (s, 1H); δ2.17–2.31 (m, 2H); δ3.87 (s, 9H); δ5.90 (s, 1H); δ6.30–6.34 (d, 1H, J = 15.68 Hz); δ6.70–6.77 (m, 3H); δ6.98–7.00 (t, 1H, J = 6.44 Hz); δ7.17 (s, 1H); δ7.50–7.54 (d, 1H, J = 15.68 Hz); δ7.64–7.62 (t, 1H, J = 7 Hz); δ8.25–8.26 (d, 1H); δ8.43 (s, 1H); δ12.39 (s, 1H). ^{13}C NMR (DMSO, 100 MHz) δ29.88; 30.07; 47.77; 55.88; 59.64; 60.12; 104.97; 112.66; 118.02; 121.45; 130.45; 139.09; 139.51; 145.65; 153.12; 153.73; 164.29; 178.07. MS 473.4 $[M+H]^+$.

5.2.1.12. 5.2.12. (E)-N-(2-methyl-1-(3-pyridin-2-ylureido)propyl)-3-(3,4,5-trimethoxyphenyl) acrylamide (382). ^{1}H NMR (400 MHz, DMSO-d_6) δ0.95–0.99 (m, 6H); δ2.21–2.24 (m, 1H); δ3.68 (s, 3H); δ3.81 (s, 6H); δ6.02–6.04 (m, 1H); δ6.61–6.64 (d, 1H, J = 15.68 Hz); δ6.90 (s, 2H); δ7.08–7.12 (dd, 1H, J = 6.44 Hz and 5.04 Hz); δ7.18–7.20 (d, 1H, J = 8.4 Hz); δ7.36–7.40 (d, 1H, J = 15.68 Hz); δ7.78–7.80 (m, 1H); δ8.24–8.25 (m, 1H); δ8.50–8.52 (m, 1H, J = 7.84 Hz); δ10.70 (s, 1H); δ12.16–12.18 (d, 1H, J = 8.12 Hz). ^{13}CNMR (DMSO, 100 MHz) δ17.72; 31.19; 55.82; 60.09; 65.49; 104.85; 112.73; 118.05; 139.19; 139.34; 145.62; 153.08; 153.74; 164.35; 179.49. MS 445.2 $[M+H]^+$.

5.2.1.13. (E)-N-(2-methyl-1-(3-phenylureido)propyl)-3-(3,4,5-trimethoxy-phenyl) acrylamide (383). ^{1}H NMR (400 MHz, DMSO-d_6) δ0.93–0.95 (m, 6H); δ2.20 (m, 1H); δ3.69 (s, 3H); δ3.82 (s, 6H); δ5.86 (m, 1H); δ6.78–6.80 (d, 1H); δ6.92 (s, 2H); δ7.11–7.13 (m, 1H); δ7.30–7.54 (m, 6H); δ7.97 (s, 1H); δ8.30 (m, 1H); δ9.91 (m, 1H). MS 444.2 $[M+H]^+$.

5.2.1.14. 5.2.14. N-(cyclopropyl(3-pyridin-2-ylthioureido)methyl)cinnamamide (384). ^{1}H NMR (400 MHz, DMSO-d_6) δ0.93–0.95 (m, 6H); δ1.91–2.29 (m, 4H); δ3.68–3.71 (m, 1H); δ3.82 (s, 6H); δ6.62–6.65 (d, 1H, J = 16 Hz); δ7.00–7.47 (m, 4H); δ7.56–7.58 (m, 2H); δ7.70–7.80 (m, 1H); δ8.23–8.24 (m, 1H); δ10.86–10.87 (m, 1H); δ12.47–12.49 (m, 1H). ^{13}C NMR (DMSO, 100 MHz) δ21.54; 33.90; 45.93; 68.88; 112.84; 118.28; 119.50; 128.15; 128.84; 129.83; 134.87; 139.29; 141.31; 145.74; 153.59; 164.29; 177.40. MS 353.2 $[M+H]^+$.

5.2.1.15. N-(3-methyl-1-(3-phenylthioureido)butyl)cinnamamide (386). ^{1}H NMR (400 MHz, DMSO-d_6) δ0.91–0.92 (m, 6H); δ1.67–1.73 (m, 3H); δ6.03 (s, 1H); δ6.66 (s, 1H); δ7.10–7.13 (t, 1H); δ7.30–7.60 (m, 10H); δ7.96 (s, 1H); δ8.56 (s, 1H); δ9.67 (s, 1H). MS 368.2 $[M+H]^+$.

5.2.1.16. N-(3,3-dimethyl-1-(3-phenylthioureido)butyl)cinnamamide (387). ^{1}H NMR (400 MHz, DMSO-d_6) δ0.92–0.95 (m, 9H); δ1.78 (m, 2H); δ6.06 (s, 1H); δ6.60–6.64 (d, 1H); δ7.10–7.13 (t, 1H); δ7.31–7.57 (m, 10H); δ7.97 (s, 1H); δ8.65 (s, 1H); δ9.71 (s, 1H). MS 382.2 $[M+H]^+$.

5.2.1.17. N-(2,2-dimethyl-1-(3-phenylthioureido)propyl)cinnamamide (388). ^{1}H NMR (400 MHz, DMSO-d_6) δ0.98 (m, 9H); δ6.15 (s, 1H); δ6.69–6.72 (d, 1H, J = 13.44 Hz); δ7.11–7.15 (t, 1H); δ7.32–7.59 (m, 10H); δ7.63–7.67 (d, 1H); δ8.17 (s, 1H); δ9.86 (s, 1H). ^{13}CNMR (DMSO, 100 MHz) δ25.58; 36.47; 66.16; 121.82; 122.20; 122.92; 124.28; 127.56; 127.81; 128.55; 128.99; 129.53; 134.90; 139.13; 139.34; 165.93; 180.52. MS 368.2 $[M+H]^+$.

5.2.1.18. N-(cyclopropyl(3-phenylthioureido)methyl)cinnamamide (389). ^{1}H NMR (400 MHz, DMSO-d_6) δ1.89–2.19 (m, 4H); δ3.57–3.58 (m, 1H); δ6.58–6.62 (t, 1H); δ7.07–7.11 (t, 1H); δ7.20–7.54 (m, 10H); δ7.69–7.71 (dd, 2H); δ9.11 (d, 1H); δ10.01 (s, 1H). MS 352.1 $[M+H]^+$.

5.2.1.19. N-(2-methyl-1-(3-phenylthioureido)propyl)cinnamamide (390). ^{1}H NMR (400 MHz, DMSO-d_6) δ0.92–0.94 (m, 6H); δ2.22 (s, 1H); δ5.83 (s, 1H); δ6.70 (d, 1H); δ7.09–7.13 (t, 1H); δ7.31–7.58 (m, 10H); δ7.85 (s, 1H); δ8.43 (s, 1H); δ9.77 (s, 1H). MS 354.1 $[M+H]^+$.

5.2.1.20. (E)-N-(3-methyl-1-(3-methylthioureido)butyl)-3-(3,4,5-trimethoxy-phenyl)acrylamide (391). ^{1}H NMR (400 MHz, DMSO-d_6) δ0.94–0.97 (m, 7H); δ1.66–1.70 (m, 3H); δ2.93 (s, 3H); δ3.75 (s, 3H); δ3.78 (s, 6H); δ5.95–5.99 (d, 1H); δ6.64–6.68 (d, 1H, J = 16 Hz); δ6.97 (s, 2H); δ7.47–7.52 (d, 1H, J = 16 Hz); δ8.01 (s, 1H); δ8.74 (t, 1H). ^{13}CNMR (DMSO, 100 MHz) δ21.89; 22.45; 24.34; 31.44; 43.99; 58.84; 60.11; 105.00; 121.01; 130.33; 138.79; 141.21; 153.58; 166.22; 183.55. MS 396.3 $[M+H]^+$.

5.2.1.21. (E)-N-(2,2-dimethyl-1-(3-o-tolylthioureido)propyl)-3-(3,4,5-trimethoxyphenyl)acrylamide (392). ^{1}H NMR (400 MHz, DMSO-d_6) δ0.94 (m, 9H); δ2.19 (s, 3H); δ3.68 (s, 3H); δ3.81 (s, 6H);

Table 6
The results of 2D ^{13}C, ^{1}H COSY(HMQC) spectra of compounds 379, 405,397 and 407.

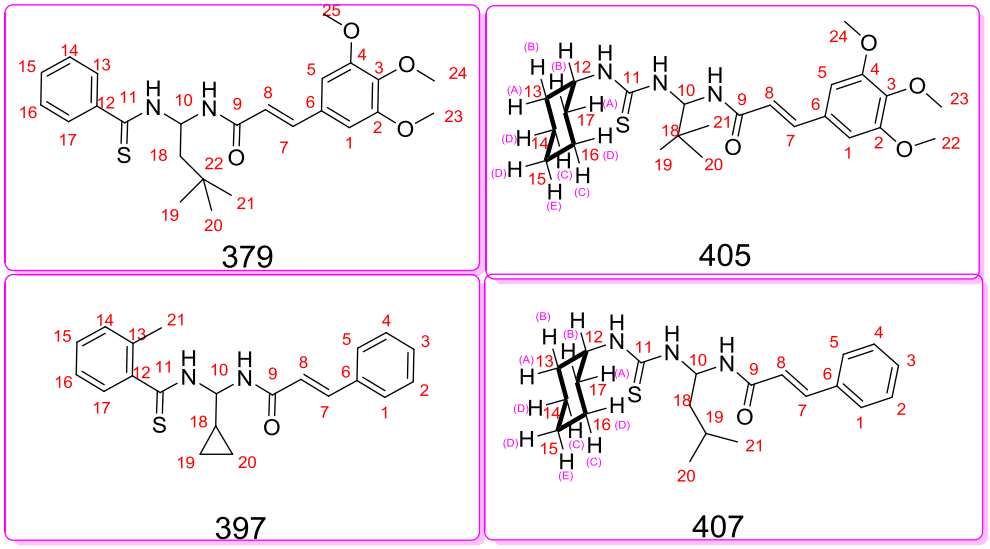

Assign.	379		405		397		407	
	δc (ppm)	δH (ppm)	δC (ppm)	δH (ppm)	δc (ppm)	δH (ppm)	δC (ppm)	δH (ppm)
C1	105.49	6.92	104.96	6.95	128.92	7.41	128.84	7.41
C2	153.60	–	152.99	–	127.68	7.53	127.52	7.56
C3	130.5	–	130.43	–	134.35	7.21	134.58	7.58
C4	153.60	–	152.99	–	127.68	7.53	127.52	7.56
C5	105.49	6.92	104.96	6.95	128.92	7.41	128.84	7.41
C6	130.9	–	130.4	–	129.97	–	129.56	–
C7	139.3	7.35	138.72	7.44	140.93	7.55	139.40	7.50
C8	121	6.60	121.30	6.73	120.45	6.72	121.17	6,67
C9	164.98	–	164.45	–	166.20		165.14	–
C10	59.69	6.08	52.16	6.95	62.50	5.99	52.48	4.01
C11	179.42	–	181.00	–	178.89	–	179.33	–
C12	139.92	–	20.07	2.04	134.34	–	57.25	–
C13	123.45	7.49	24.27	1.7(A), 1.31(B)	139.01	–	24.28	1.65 (A), 1.22(B)
C14	129.09	7.33	32.15	1.92(C), 1.23(D)	129.87	7.19	31.82	1.85(C), 1.18(D)
C15	124.75	7.12	25.11	1.58(E), 1.23(D)	128.82	7.14	25.10	1.50(E), 1.18(D)
C16	129.09	7.33	32.15	1.92(C), 1.23(D)	125.73	7.15	24.28	1.65 (A), 1.22(B)
C17	123.45	7.49	24.27	1.7(A), 1.31(B)	126.23	7.12	31.82	1.85(C), 1.18(D)
C18	48.11	1.79	35.77	–	51.70	3.76	42.19	1.64
C19	30.25	0.96	25.38	0.89	33.04	2.13,2.00	32.20	1.21
C20	30.25	0.96	25.38	0.89	21.94	2.20,1.99	21.80	0.89
C21	30.25	0.96	25.38	0.89	17.49	2.14	21.80	0.89
C22	14.50	–	55.80	3.87				
C23	56.35	3.82	59.99	3.74				
C24	60.62	3.69	55.80	3.87				
C25	56.35	3.82						

δ6.19 (s, 1H); δ6.61–6.65 (d, 1H); δ6.92 (s, 2H); δ7.16–7.52 (m, 6H); δ8.61 (d, 1H); δ9.46 (s, 1H). ^{13}CNMR (DMSO, 100 MHz) δ17.78; 25.54; 36.73; 55.82; 60.09; 66.37; 104.86; 121.73; 126.04; 126.34; 128.07; 130.36; 130.54; 134.48; 137.40; 138.58; 139.17; 153.08; 163.87; 181.75. MS 472.3 $[M+H]^+$.

5.2.1.22. (E)-N-(cyclopropyl(3-o-tolylthioureido)methyl)-3-(3,4,5-trimethoxyphenyl)acrylamide (393). ^{1}H NMR (400 MHz, DMSO-d_6) δ0.38–0.46 (m, 4H); δ1.42 (s, 1H); δ2.18 (s, 3H); δ3.68 (s, 3H); δ3.81 (s, 6H); δ5.72 (s, 1H); δ6.57–6.63 (d, 1H); δ6.92 (s, 2H); δ7.14–7.40 (m, 5H); δ7.76 (s, 1H); δ8.36 (s, 1H); δ9.346 (s, 1H). MS 456.3 $[M+H]^+$.

5.2.1.23. N-(3,3-dimethyl-1-(3-o-tolylthioureido)butyl)cinnamamide (394). ^{1}H NMR (400 MHz, DMSO-d_6) δ0.95 (m, 9H); δ1.69–1.80 (m, 2H); δ2.16 (s, 3H); δ6.06 (s, 1H); δ6.59–6.63 (d, 1H); δ7.13–7.24 (m, 4H); δ7.41–7.44 (m, 4H); δ7.57–7.59 (d, 3H); δ8.59 (s, 1H); δ9.24 (s, 1H). ^{13}CNMR (DMSO, 100 MHz) δ180.10, 164.64, 139.29, 134.39, 130.42, 129.63.129.01, 127.68, 126.42, 126.13, 122.96, 59.22, 48.01, 29.97, 29.68, 17.69. MS 395.9 $[M+H]^+$.

5.2.1.24. N-(3-methyl-1-(3-o-tolylthioureido)butyl)cinnamamide (395). ^{1}H NMR (400 MHz, DMSO-d6) δ0.86–0.92 (m, 6H); δ1.24–1.25 (m, 1H); δ1.67–1.68 (m, 2H); δ2.16 (s, 3H); δ6.05 (s, 1H); δ5.47–5.52 (s, 1H, N–H); δ6.06 (s, 1H); δ6.64–6.69 (m, 1H);

δ7.15–7.18 (m, 4H); δ7.41–7.43 (m, 3H); δ7.58–7.59 (d, 2H); δ8.47 (s, 1H); δ9.20 (s, 1H) δ9.95 (s, 1H, N–H). MS 381.5 $[M+H]^+$.

5.2.1.25. N-(2,2-dimethyl-1-(3-o-tolylthioureido)propyl)cinnamamide (396). ^{1}H NMR (400 MHz, DMSO-d_6) δ0.94 (m, 9H); δ2.18 (s, 3H); δ6.15 (s, 1H); δ6.71 (s, 1H); δ7.17–7.26 (m, 4H); δ7.38–7.45 (m, 4H); δ7.57–7.59 (d, 2H); δ8.19 (s, 1H). MS 382.1 $[M+H]^+$.

5.2.1.26. 5.2.26. N-(cyclopropyl(3-o-tolylthioureido)methyl)cinnamamide (397). ^{1}H NMR (400 MHz, DMSO-d_6) δ1.97–2.00 (m, 2H); δ2.08–2.32 (m, 4H); δ3.72–3.81 (m, 2H); δ5.98–6.01 (t, 1H); δ6.71–6.75 (d, 1H, J = 16 Hz); δ7.15–7.16 (m, 4H); δ7.40–7.43 (m, 3H); δ7.53–7.60 (m, 3H); δ9.10 (s, 1H); δ9.62 (s, 1H). ^{13}CNMR (DMSO, 100 MHz) δ17.49; 21.94; 33.04; 51.70; 60.09; 62.50; 120.45; 125.73; 126.32; 127.68; 128.82; 128.92; 129.87; 129.97; 134.35; 134.90; 139.01; 140.93; 166.20; 178.89. MS 366.2 $[M+H]^+$. The results of 2D ^{13}C, ^{1}H COSY(HMQC) spectra of compound 397 was shown in Table 6.

5.2.1.27. (E)-N-(1-(3-(4-methoxyphenyl)thioureido)-2-methylpropyl)-3-(3,4,5-trimethoxyphenyl)acrylamide (402). ^{1}H NMR (400 MHz, DMSO-d_6) δ0.91–0.98 (m, 6H); δ2.18 (s, 1H); δ3.68 (s, 3H); δ3.74 (s, 3H); δ3.81 (s, 6H); δ5.86 (s, 1H); δ6.60–6.64 (d, 1H); δ6.90–6.92 (d, 2H); δ7.32–7.38 (m, 3H); δ8.30 (s, 1H); δ9.60 (s, 1H). ^{13}C NMR (DMSO, 100 MHz) δ18.12; 31.68; 55.23; 55.84; 60.11; 64.99; 104.96; 113.89; 125.50; 130.29; 130.59; 131.39; 138.68; 139.38; 153.07; 156.45; 164.55; 180.34. MS 474.2 $[M+H]^+$.

5.2.1.28. (E)-N-(1-(3-cyclohexylthioureido)-3-methylbutyl)-3-(3,4,5-trimethoxyphenyl)acrylamide (404). ^{1}H NMR (400 MHz, CCl_3D-*d*) δ0.90–0.93 (m, 6H); δ1.29–1.35 (m, 5H); δ1.61–1.77 (m, 5H); δ1.92–2.15 (m, 2H); δ3.89 (m, 9H); δ4.09–4.11 (m, 1H); δ5.44–5.48 (m, 1H); δ6.19 (s, 1H); δ6.47–6.51 (d, 1H); δ6.76–6.85 (m, 2H); δ7.27–7.34 (d, 1H); δ7.57–7.61 (d, 1H); δ8. 27 (s, 1H). MS 464.4 $[M+H]^+$.

5.2.1.29. 5.2.29. (E)-N-(1-(3-cyclohexylthioureido)-2,2-dimethylpropyl)-3-(3,4,5-trimethoxyphenyl)acrylamide (405). ^{1}H NMR (400 MHz, DMSO-*d6*) δ0.89 (s, 9H); δ1.20–1.31 (m, 7H); δ1.57–1.60 (d, 1H); δ1.67 (s, 2H); δ1.91 (s, 2H) δ2.04 (s, 1H); δ3.79 (s, 3H); δ3.86 (s, 1H); δ5.05–4.09 (m, 1H); δ6.01–6.04 (s, 1H); δ6.67–6.74 (d, 1H); δ6.95 (s, 2H); δ7.21–7.25 (d, 1H); δ7.24–7.26 (d, 1H); δ7.42–7.45 (d, 1H); δ7.68–7.70 (d, 1H); δ8.16 (s, 1H). ^{13}C NMR (DMSO, 100 MHz) δ181.00; 164.45; 152.99; 139.32; 138.72; 130.43; 121.30; 104.96; 65.50; 59.99; 59.61; 55.80; 52.16; 35.77; 32.15; 31.98; 25.38; 25.11; 24.27; 13.98. MS 464.4 $[M+H]^+$. The results of 2D ^{13}C, ^{1}H COSY(HMQC) spectra of compound 405 was shown in Table 6.

5.2.1.30. (E)-N-(1-(3-cyclohexylthioureido)-2-methylpropyl)-3-(3,4,5-trimethoxyphenyl)acrylamide (406). ^{1}H NMR (400 MHz, -*d*) δ1.02–1.34 (m, 11H); δ1.63–2.05 (m, 6H); δ3.87–3.89 (m, 9H); δ4.09–4.11 (m, 1H); δ5.14–5.18 (m, 1H); δ6.17 (s, 1H); δ6.55–6.59 (d, 1H); δ6.74–6.78 (m, 2H); δ7.57–7.61 (d, 1H); δ8.02 (s, 1H). MS 450.2 $[M+H]^+$.

5.2.1.31. N-(1-(3-cyclohexylthioureido)-3-methylbutyl)cinnamamide (407). ^{1}H NMR (400 MHz, DMSO-d_6) δ0.88–0.89 (m, 6H); δ1.03–1.33 (m, 6H); δ1.53–1.66 (m, 7H); δ1.82–1.91 (m, 2H); δ4.01 (s, 1H); δ6.63–6.67 (d, 1H, J = 15.68 Hz); δ7.37–7.45 (m, 5H); δ7.48–7.52 (d, 1H, J = 15.68 Hz); δ7.56–7.62 (d, 2H, J = 6.76 Hz); δ7.76 (s, 1H); δ8.69 (s, 1H). ^{13}CNMR (DMSO, 100 MHz) δ21.80; 22.22; 24.24; 24.28; 25.10; 31.82; 32.20; 42.19; 52.48; 57.25; 121.17; 127.52; 128.84; 134.58; 139.40; 165.14; 179.33. MS 374.3 $[M+H]^+$. The results of 2D ^{13}C, ^{1}H COSY(HMQC) spectra of compound 407 was shown in Table 6.

5.2.1.32. N-(1-(3-cyclohexylthioureido)-2-methylpropyl)cinnamamide (408). ^{1}H NMR (400 MHz, DMSO-d_6) δ0.87–0.92 (m, 6H); δ1.10–1.29 (m, 6H); δ1.56–1.87 (m, 5H); δ2.12 (s, 1H); δ3.98 (s, 1H); δ6.68–6.72 (d, 1H); 7.39–7.44 (q, 4H); δ7.57–7.66 (d, 2H). MS 360.3 $[M+H]^+$.

5.2.1.33. N-(1-(3-cyclohexylthioureido)-2,2-dimethylpropyl)cinnamamide (409). ^{1}H NMR (400 MHz, DMSO-d_6) δ0.98–1.35 (m, 14H); δ1.57–2.10 (m, 5H); δ4.10–4.12 (d, 1H); δ5.19–5.24 (m, 1H); δ5.61 (s, 1H); δ6.03–6.05 (s, 1H); δ6.47–6.59 (d, 1H); δ7.35–7.38 (t, 2H); δ7.50–7.54 (d, 2H); δ7.65–7.70 (d, 2H). ^{13}C NMR (DMSO, 100 MHz) δ180.99; 164.67; 139.15; 134.85; 129.33; 128.82; 127.39; 122.03; 65.58; 52.10; 35.82; 32.14; 31.99; 25.37; 25.10; 24.24. MS 374.3 $[M+H]^+$.

6. Biological evaluations

6.1. Colorimetric determination of ATPase activity

The assay procedure was adopted from previous reports with some modifications [26]where indicated. Stock solutions of malachite green (0.1% w/v), polyvinyl alcohol (2.3% w/v), and ammonium molybdate tetrahydrate (1% w/v in 1 M HCl) were prepared and mixed with water at the ratio of 2:1:1:2 to prepare the malachite green reagent, which is stable at room temperature for at least 2 h. After its colour changing from dark brown to yellow, the reagent should be filtrated through a 0.22-μM filtration membrane prior to use. ATP, malachite green, polyvinyl alcohol and ammonium molybdate tetrahydrate were purchased from SIGMA and used without further purification.

For compound screening, an aliquot of a master mixture of DnaK:DnaJ (2.0 μM:3.5 μM) prepared in assay buffer (0.017% Triton X-100, 100 mM Tris–HCl, 20 mM KCl, and 6 mM $MgCl_2$, pH 7.4) was added into each well of a 96-well plate (14 μL per well). To this solution, 1 μL of either one of the test compounds (5 mM) or DMSO was added, and the plate was shaken for 10 min and incubated for 30 min at 37 °C.

Ten microlitres of 2.5 mM ATP was added to start the reaction. Thus, the final reaction volume was 25 μL, and the concentration of the tested compounds was 200 μM. After 3 h of incubation at 37 °C, 80 μL of the malachite green reagent was added into each well, and the plates were shaken gently. Immediately following this step, 10 μL of 34% sodium citrate was added to terminate the nonenzymatic hydrolysis of ATP. After the samples were mixed thoroughly and incubated at 37 °C for 15 min, the OD_{620} was measured using a SpectraMax M5 (Molecular Devices, Sunnyvale, CA, USA).

6.2. Screening of resistance reversal agents

The breast cancer cell lines BT474 and BT/LapR$^{1.0}$ were selected for the *in vitro* evaluation of the cell viability and coefficient of drug interaction (CDI) of the thiourea derivatives. The epidermal growth factor (EGFR: ErbB-1, ErbB-2) tyrosine kinase inhibitor lapatinib (10 mM in DMSO, BioVision, Cat: 1624-100, Lot: 50324) was used as the positive control. The cell viability was measured using the CellTiter-Glo® kit (Promega, Part: G755B, Lot: 32513501, EXP: 2014-05). The cells were digested in 1 mL of 0.25% trypsin (Gibco) supplemented with 2 mL of medium (containing 10% FBS, Gibco) and seeded (1×10^5 cells/mL, 50 μL/well, 5000 cells/well) into 96-well plates. The plates were incubated for 24 h at 37 °C. The serially diluted compounds and control were added into each well, and the cells were incubated for 72 h at 37 °C. A volume of the CellTiter-Glo Reagent (50 μL) equal to the volume of the cell culture medium

present in each well was added. The plates were shaken for 3 min on an orbital shaker to induce cell lysis. To stabilize the luminescent signal, the plate was incubated at room temperature for 10 min. The luminescent signal was measured, and the data were normalized to that obtained for the control group. The cell viability was determined based on the luminescence: cell viability (%) = $RLU_{experimental\ group}/RLU_{blank\ group} \times 100\%$. Simultaneously, the coefficient of drug interaction (CDI) [25]was used to characterize the interactions as synergism, additivity or antagonism: CDI = AB/(A × B) × 100% (A, B and AB refer to the percentage inhibition calculated by cell viability). If CDI < 1, the tested compounds exhibited a synergistic effect with lapatinib, and significant synergy with lapatinib was defined as CDI < 0.7.

Acknowledgements

This work was supported by Grant No. 81473139 to Wu Zhong from the National Natural Science Foundation of China and the State Key Laboratory of Toxicology and Medical Countermeasures.

Appendix A. Supplementary data

Supplementary data related to this article can be found at http://dx.doi.org/10.1016/j.ejmech.2016.04.042.

References

[1] W.B. Pratt, D.O. Toft, Regulation of signaling protein function and trafficking by the hsp90/hsp70-based chaperone machinery, Exp. Biol. Med. (Maywood) 228 (2003) 111–133.
[2] J.C. Young, J.M. Barral, F. Ulrich Hartl, More than folding: localized functions of cytosolic chaperones, Trends Biochem. Sci. 28 (2003) 541–547.
[3] M.P. Mayer, B. Bukau, Hsp70 chaperones: cellular functions and molecular mechanism, Cell Mol. Life Sci. 62 (2005) 670–684.
[4] E. Meimaridou, S.B. Gooljar, J.P. Chapple, From hatching to dispatching: the multiple cellular roles of the Hsp70 molecular chaperone machinery, J. Mol. Endocrinol. 42 (2009) 1–9.
[5] M.Y. Sherman, V.L. Gabai, Hsp70 in cancer: back to the future, Oncogene 34 (32) (2015) 4153–4161.
[6] Y.L. Tsai, Y. Zhang, C.C. Tseng, R. Stanciauskas, F. Pinaud, A.S. Lee, Characterization and mechanism of stress-induced translocation of 78-kilodalton glucose regulated protein (GRP78) to the cell surface, J. Biol. Chem. 290 (13) (2015) 8049–8064.
[7] A.R. Stankiewicz, G. Lachapelle, C.P. Foo, S.M. Radicioni, D.D. Mosser, Hsp70 inhibits heat-induced apoptosis upstream of mitochondria by preventing Bax translocation, J. Biol. Chem. 280 (2005) 38729–38739.
[8] Z.N. Demidenko, C. Vivo, H.D. Halicka, C.J. Li, K. Bhalla, E.V. Broude, M.V. Blagosklonny, Pharmacological induction of Hsp70 protects apoptosis-prone cells from doxorubicin: comparison with caspase-inhibitor- and cycle-arrest-mediated cytoprotection, Cell Death Differ. 13 (2006) 1434–1441.
[9] V. Jendrossek, R. Handrick, Membrane targeted anticancer drugs: potent inducers of apoptosis and putative radiosensitisers, Curr. Med. Chem. Anti-cancer Agents 3 (2003) 343–353.
[10] E. Schmitt, M. Gehrmann, M. Brunet, G. Multhoff, C. Garrido, Intracellular and extracellular functions of heat shock proteins: repercussions in cancer therapy, J. Leukoc. Biol. 81 (2007) 15–27.
[11] K. Ruchalski, H. Mao, Z. Li, Z. Wang, S. Gillers, Y. Wang, D.D. Mosser, V. Gabai, J.H. Schwartz, S.C. Borkan, Distinct hsp70 domains mediate apoptosis-inducing factor release and nuclear accumulation, J. Biol. Chem. 281 (2006) 7873–7880.
[12] H.E. Kim, X. Jiang, F. Du, X. Wang, PHAPI, CAS, and Hsp70 promote apoptosome formation by preventing Apaf-1 aggregation and enhancing nucleotide exchange on Apaf-1, Mol. Cell 30 (2008) 239–247.
[13] J.S. Guo, J.F. Chau, X.Z. Shen, C.H. Cho, J.M. Luk, M.W. Koo, Over-expression of inducible heat shock protein 70 in the gastric mucosa of partially sleep-deprived rats, Scand. J. Gastroenterol. 39 (2004) 510–515.
[14] Q. Pang, W. Keeble, T.A. Christianson, G.R. Faulkner, G.C. Bagby, FANCC interacts with Hsp70 to protect hematopoietic cells from IFN-gamma/TNF-alpha-mediated cytotoxicity, EMBO J. 20 (2001) 4478–4489.
[15] Q. Pang, T.A. Christianson, W. Keeble, T. Koretsky, G.C. Bagby, The anti-apoptotic function of Hsp70 in the interferon-inducible double-stranded RNA-dependent protein kinase-mediated death signaling pathway requires the Fanconi anemia protein, FANCC, J. Biol. Chem. 277 (2002) 49638–49643.
[16] S. Singh, A. Suri, Targeting the testis-specific heat-shock protein 70-2 (HSP70-2) reduces cellular growth, migration, and invasion in renal cell carcinoma cells, Tumour Biol. 35 (2014) 12695–12706.
[17] X. Lu, L. Xiao, L. Wang, D.M. Ruden, Hsp90 inhibitors and drug resistance in cancer: the potential benefits of combination therapies of Hsp90 inhibitors and other anti-cancer drugs, Biochem. Pharmacol. 83 (2012) 995–1004.
[18] A. Yerlikaya, E. Okur, S. Eker, N. Erin, Combined effects of the proteasome inhibitor bortezomib and Hsp70 inhibitors on the B16F10 melanoma cell line, Mol. Med. Rep. 3 (2010) 333–339.
[19] Y. Wang, S.R. McAlpine, Combining an Hsp70 inhibitor with either an N- or C-terminal Hsp90 inhibitor produces mechanistically distinct phenotypes, Org. Biomol. Chem. 13 (2015) 3691–3698.
[20] J. Liu, K.L. He, X. Li, R.J. Li, C.L. Liu, W. Zhong, S. Li, SAR, cardiac myocytes protection activity and 3D-QSAR studies of salubrinal and its potent derivatives, Curr. Med. Chem. 19 (2012) 6072–6079.
[21] A.R. Katritzky, X. Lan, J.Z. Yang, O.V. Denisko, Properties and synthetic utility of N-Substituted benzotriazoles, Chem. Rev. 98 (1998) 409–548.
[22] A.J. Massey, D.S. Williamson, H. Browne, J.B. Murray, P. Dokurno, T. Shaw, A.T. Macias, Z. Daniels, S. Geoffroy, M. Dopson, P. Lavan, N. Matassova, G.L. Francis, C.J. Graham, R. Parsons, Y. Wang, A. Padfield, M. Comer, M.J. Drysdale, M. Wood, A novel, small molecule inhibitor of Hsc70/Hsp70 potentiates Hsp90 inhibitor induced apoptosis in HCT116 colon carcinoma cells, Cancer Chemother. Pharmacol. 66 (2010) 535–545.
[23] H.J. Cho, H.Y. Gee, K.H. Baek, S.K. Ko, J.M. Park, H. Lee, N.D. Kim, M.G. Lee, I. Shin, A small molecule that binds to an ATPase domain of Hsc70 promotes membrane trafficking of mutant cystic fibrosis transmembrane conductance regulator, J. Am. Chem. Soc. 133 (2011) 20267–20276.
[24] D. Wang, Z. Wang, B. Tian, X. Li, S. Li, Y. Tian, Two hour exposure to sodium butyrate sensitizes bladder cancer to anticancer drugs, Int. J. Urol. 15 (2008) 435–441.
[25] C. Soica, C. Oprean, F. Borcan, C. Danciu, C. Trandafirescu, D. Coricovac, Z. Crainiceanu, C.A. Dehelean, M. Munteanu, The synergistic biologic activity of oleanolic and ursolic acids in complex with hydroxypropyl-gamma-cyclodextrin, Molecules 19 (2014) 4924–4940.
[26] L. Chang, E.B. Bertelsen, S. Wisen, E.M. Larsen, E.R. Zuiderweg, J.E. Gestwicki, High-throughput screen for small molecules that modulate the ATPase activity of the molecular chaperone DnaK, Anal. Biochem. 372 (2008) 167–176.